Expanding Continuous Tuning Range of a CW Single-Frequency Laser by Combining an Intracavity Etalon With a Nonlinear Loss

Pixian Jin, Huadong Lu, Qiwei Yin, Jing Su, and Kunchi Peng

***Abstract*—Combining intracavity etalon (IE) locked on a laser oscillating mode with a deliberately introduced nonlinear loss, the tuning range of a continuous-wave (CW) single-frequency laser is significantly expanded to transcend the traditional limitation of a free spectral range (FSR) of IE. Due to the action of the nonlinear loss, the frequency of laser oscillating mode can be continuously and smoothly tuned without any mode-hopping in a tuning range much larger than FSR of IE. We theoretically analyze the physical mechanism behind the influence of nonlinear loss on the tuning range expansibility of the laser and experimentally demonstrated the effectiveness of the presented method. By means of this method, the ultrawide continuous frequency scanning range of 222.4 GHz at 532 nm is implemented. The theoretical analysis and the experimental results are in good agreement.**

***Index Terms*—Tunable laser, continuous frequency-tuning, nonlinear loss, sing mode.**

I. Introduction

ALL-SOLID-STATE continuous wave (CW) single-frequency lasers with intrinsic merits of low intensity noise, high beam quality and high stability have served for quantum optics and quantum information [1]–[3], atom cooling and trapping, optical frequency standards [4], [5] and so on. For lots of applications such as atom cooling and trapping as well as optical frequency standards, the broadband tuning range and continuous tuning ability of CW single-frequency lasers are desired for matching wavelengths of lasers to the absorption lines of the atoms. The common laser tuning method is to employ a mode-selection element, such as an intracavity etalon (IE). Generally, the broadband tuning range can be achieved by changing the effective optical path of IE and continuous tuning of a laser can be implemented by scanning the effective resonant length after the transmission peak of IE is locked to an oscillating mode of the laser. In 1992, Harrison *et al.* obtained a tunable single-frequency laser with tuning range over 50 GHz by rotating the incident angle of IE [6]. In 2015, D. Radnatarov *et al.* reported a quasi-continuously frequency tunable laser with tuning range of 240 GHz at 532 nm, which is achieved by locking two IEs with different thickness and automatic stitching several smooth frequency scanning ranges (18 GHz @ 532 nm) [7]. Besides rotating the incident angle of IE, frequency tuning of the laser can also be implemented by scanning the temperature of IE. In 2013, our group demonstrated a tunable single-frequency green laser with the output power over 10 W and tuning range over 24 GHz by scanning temperatures of IE and gain medium [8]. A tunable single-frequency 1064 nm laser with tuning range of 17.2 GHz and a tunable single-frequency Ti:sapphire laser with continuous tuning range of 20 GHz were achieved by utilizing the electro-optic IE as the tuning elements in 2008 [9] and in 2017 [10], respectively. In all above mentioned lasers, however, the maximal continuous tuning ranges were restricted within a free spectral range (FSR) of IE. An effective solution to this issue would be deliberately introducing a nonlinear loss to the laser resonator. It has been proved that the nonlinear loss of the laser oscillating mode is a half of that of non-oscillating modes in [11], [12], and a mode-hop-free tuning range of more than 80 GHz for second-harmonic wave (SHW) laser around the wavelength of gain center was achieved. In contrast to the previous study, in this letter, our emphasis is combining the IE and a nonlinear loss to expand the continuous tuning range of single-frequency laser, which paves the way for expanding the tuning range of a CW single-frequency laser beyond the traditional restriction of a FSR of IE. In the following, the physical mechanism of the scheme is firstly analyzed and then an experimental verification is presented. Using a CW single-frequency and frequency-doubling Nd:YVO_4 laser, the continuous frequency-tuning range of 222.4 GHz at 532 nm is achieved successfully by combining an intracavity locked etalon and a delibrately introduced nonlinear loss, which is, to our best knowledge, the broadest continuous tuning range accomplished only by simply scanning the cavity length after the IE is locked.

Manuscript received August 10, 2017; revised December 3, 2017; accepted December 4, 2017. Date of publication December 7, 2017; date of current version December 28, 2017. This work was supported in part by the Key Project of the Ministry of Science and Technology of China under Grant 2016YFA0301401 and in part by the fund for Shanxi "1331 Project" Key Subjects Construction. *(Corresponding author: Huadong Lu.)*

The authors are with the State Key Laboratory of Quantum Optics and Quantum Optics Devices, Collaborative Innovation Center of Extreme Optics, Institute of Opto-Electronics, Shanxi University, Taiyuan 030006, China (e-mail: jinpeixian2008@163.com; luhuadong@sxu.edu.cn; yinqiweiouc@126.com; jingsu@sxu.edu.cn; kcpeng@sxu.edu.cn).

Color versions of one or more of the figures in this paper are available online at http://ieeexplore.ieee.org.

Digital Object Identifier 10.1109/JSTQE.2017.2781133

II. Principle Analysis

For a single-frequency fundamental-wave (FW) laser, an etalon is often inserted into the ring resonator to narrow the gain linewidth and keeps single-longitude-mode (SLM) operation of

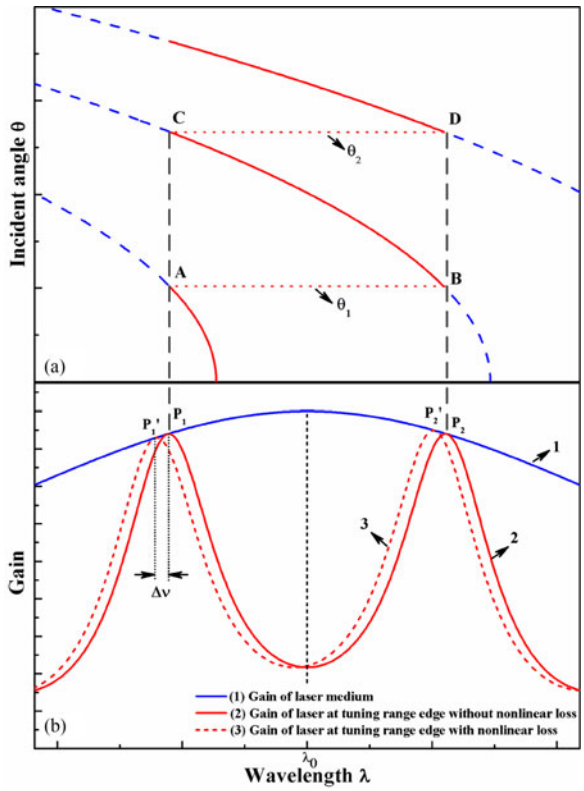

Fig. 1. (a) Theoretical prediction of the tuning curve of the IE. (b) The gain of (1) laser medium, (2) laser at tuning range edge without nonlinear loss, (3) laser at tuning range edge with nonlinear loss.

laser. Meanwhile, the frequency-tuning of the single-frequency FW laser can also be implemented by changing the effective optical path of the IE. However, the wavelength of laser will not always shift sequentially because the frequency-tuning range of FW laser is limited by FSR of the adopted IE. For instance, by adjusting the incident angle θ of IE, the output wavelength λ of laser can be finely tuned with mode-hop as shown in Fig. 1(a), where A, C and B, D are the short and long wave edges (SWE and LWE) of the tuning range, respectively. With the increasing of θ, the output wavelength λ of laser shifts to the side of short waves. When the incident angle of IE is increased to the critical angle of θ_1 corresponding to edge of the tuning range, the adjacent two transmission peaks of IE near the center wavelength of the gain medium [line 1 in Fig. 1(b)] are symmetric with respect to the center wavelength λ_0, which is shown as line 2 in Fig. 1(b). The laser gain at point P_1 is equal to that at point P_2. When the incident angle of IE is continuously increased, the mode at point P_1 hops to that at point P_2 for the latter gain is larger than the former, which corresponds to the variation of laser output wavelength from A to B in Fig. 1(a). Likewise, when the incident angle of IE is increased to another critical angle of θ_2, the output wavelength of laser from C hops to D shown in Fig. 1(a), which corresponds to a FSR of IE.

In the case without intracavity nonlinear loss element, if the transmission peak of the IE is locked to the oscillating mode of laser and the cavity length of laser resonator is continuously scanned, the continuous frequency-tuning of laser can be realized only within a FSR of IE around the center wavelength of laser medium. However, when a nonlinear loss element is deliberately introduced to the ring laser resonator, the frequency of the lasing mode can be continuously tuned by scanning the cavity length after the IE is locked, even though the incident angle of IE is rotated over the critical angles of θ_1 or θ_2. During scanning, the mode-hopping phenomenon will not occur that is because the nonlinear loss of non-oscillating modes is twice of the oscillating mode loss, so the non-oscillating mode is effectively suppressed and the difference of nonlinear losses between oscillating and non-oscillating modes is equal to the second-harmonic-generation (SHG) efficiency η [11]–[17]. At this time, the output frequency of laser can be continuously tuned without mode-hop until the gain difference of laser medium between points P_1' and P_2' reaches the value of η, which is shown as line 3 in Fig. 1(b). The gains of the laser medium g_1 and g_2 at points P_1' and P_2' are expressed respectively by,

$$g_1 = g_0 \times \frac{(\frac{\Delta\nu_H}{2})^2}{(\frac{\nu_{FSR}}{2} + \Delta\nu)^2 + (\frac{\Delta\nu_H}{2})^2} \tag{1}$$

and

$$g_2 = g_0 \times \frac{(\frac{\Delta\nu_H}{2})^2}{(\frac{\nu_{FSR}}{2} - \Delta\nu)^2 + (\frac{\Delta\nu_H}{2})^2} \tag{2}$$

where $\Delta\nu$ stands for the frequency offset from P_1 to P_1', g_0 is the gain of laser medium at center wavelength λ_0, $\Delta\nu_H$ is the gain linewidth of laser medium, ν_{FSR} is the FSR of IE. According to $g_2 - g_1 = \eta$, the maximal mode-hop-free frequency-tuning range from the point P_1 (P_2) toward higher (lower) frequency is extended,

$$\Delta\nu = \frac{(\frac{\Delta\nu_H}{2})^2}{2\nu_{FSR}} \times \frac{\eta}{\eta + L} \tag{3}$$

where L is the intracavity linear loss including the roundtrip intracavity loss and the transmission of output coupler for the FW laser, and $g_1 = \eta + L$, which is the stable oscillation condition of laser. Thus, the maximum continuous frequency-tuning range $\Delta\nu_{\max}$ of the CW single-frequency laser containing a locked IE and a nonlinear loss element equals to,

$$\Delta\nu_{\max} = \nu_{FSR} + 2\Delta\nu = \nu_{FSR} + \frac{(\frac{\Delta\nu_H}{2})^2}{\nu_{FSR}} \times \frac{\eta}{\eta + L} \tag{4}$$

III. Experimental Setup

The theoretical prediction is confirmed by an all-solid-state CW single-frequency and frequency-doubling laser containing a locked IE and a nonlinear loss element. The configuration of designed laser is shown in Fig. 2. A fiber coupled laser diode (LD) with output power of 8.02 W at 808 nm act as the pump source, who is installed in laser controller (LC). The pump beam output from the fiber with core diameter of 400 μm and numerical aperture (N.A.) of 0.22 is coupled into the ring cavity by a telescope system consisting of two lenses f_1 and f_2 with the focal lengths of 30 mm and 80 mm, respectively. The bow-tie ring cavity with the length of 300 mm is constituted by four mirrors M_1–M_4. The plane mirror M_1 coated with high transmission (HT) film at

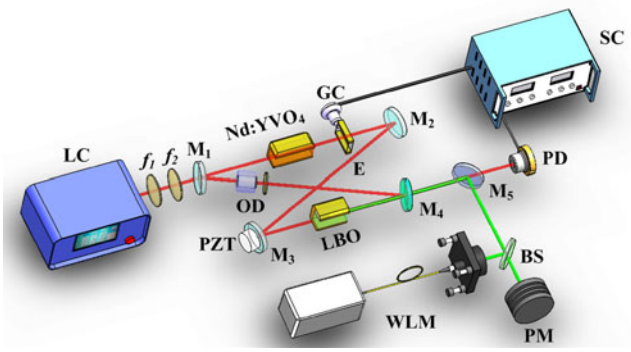

Fig. 2. Schematic diagram of super broadband tunable CW single-frequency laser. LC, laser controller; f_{1-2}, lenses; M_{1-4}, mirrors; Nd:YVO_4, Nd^{3+}-doped yttrium vanadate; LBO, lithium triborate; E, etalon; GC, galvanometer scanner; SC, servo controller; OD, optical diode; PZT, piezoelectric transducer; PD, photodetector; BS, beam spliter; PM, power meter; WLM, wavelength meter.

808 nm ($T_{808} > 95\%$) and high reflection (HR) film at 1064 nm ($R_{1064} > 99.8\%$) is used as input coupler. The plane mirror M_2 and plane-concave mirror M_3 are both coated with HR film at 1064 nm ($R_{1064} > 99.8\%$). The plane-concave mirror M_4 used as output coupler is coated with HR film at 1064 nm ($R_{1064} > 99.8\%$) and HT film at 532 nm ($T_{532} > 95\%$). The curvature radii of concave mirrors M_3 and M_4 are both 50 mm. The gain medium is a temperature controlled Nd:YVO_4 crystal (Nd^{3+}-doped yttrium vanadate with the length of 5 mm), which is positioned between M_1 and M_2. The front end-face of the gain medium is coated with antireflection (AR) films at both 808 nm and 1064 nm ($R_{808,1064} < 0.25\%$) and the second end-face is coated with AR film only at 1064 nm. To ensure the unidirectional operation of the laser, the optical diode (OD) is inserted into the resonator, which is composed by a permanent magnet surrounded terbium gallium garnet (TGG) crystal with size of $\Phi 4$ mm $\times$ 8 mm and a half-wave plate (HWP). A type-I phase-matching lithium triborate (LBO) crystal with temperature controlled to the phase-matching temperature of 146 °C is placed at the beam waist between the mirror M_3 and M_4 to obtain high SHG efficiency. The dimensions of the LBO crystal are 3 mm $\times$ 3 mm $\times$ 20 mm. The Nd:YVO_4, TGG, LBO crystals are both designed with a wedge end face to remove their etalon effects to guarantee that the laser frequency can be tuned broadly. In order to realize the continuously frequency tuning of laser, an electro-optic IE made of $LiNO_3$ crystal with thickness of 1 mm is inserted into the cavity. The IE is adhered to the axis of a galvanometer scanner (GC) to finely tune the output frequency of laser by rotating its incident angle. A long piezoelectric transducer (PZT, HPSt 150/14–10/55, Piezomechanik GmbH) used to mount mirror M_3 can continuously scan the length of resonator by changing voltage.

The 1064 nm laser leaked from the output coupler is separated by a dichroic mirror M_5 from the main output 532 nm laser and then is used to lock the electro-optic IE with a phase-lock system consisting of a photodetector (PD, ETX-500, JDSU Corporation) and a servo controller (SC). A fractional of the output 532 nm laser is reflected by a beam spliter (BS) and coupled into a wavelength meter (WLM, WS6, High Finesses Laser

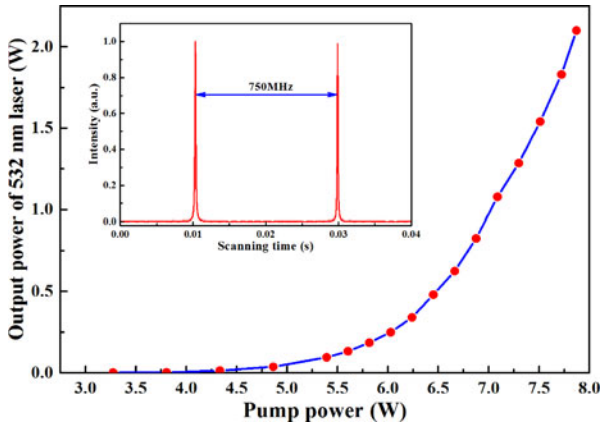

Fig. 3. The output power of the tunable single-frequency laser and SLM curve.

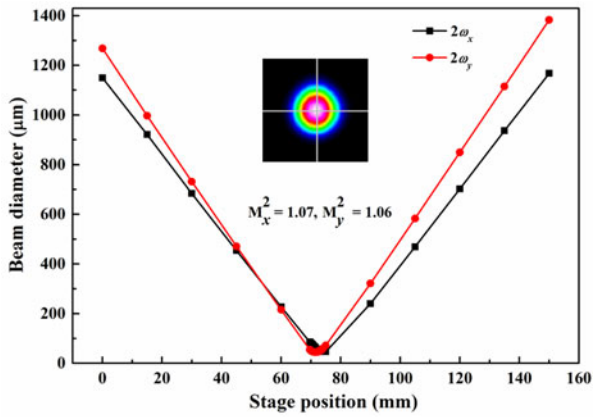

Fig. 4. Measured beam quality of the output laser.

and Electronic System) to distinguish the output wavelength (or frequency) of laser and record the frequency-tuning range. The residual part of the main output 532 nm laser transmitted through BS is detected by a power meter (PM, LabMax-TOP, Coherent).

IV. Experimental Results

In the experiment, because the output coupler was coated with HR film at FW and HT films at SHW, the main output laser was 532 nm, and the output power of the laser at 532 nm versus the pump power was recorded as shown in Fig. 3. When the pump power was 7.87 W, the maximal output power of 2.1 W at 532 nm was obtained. The threshold pump power and optical-optical conversion efficiency were 3.27 W and 26.7%, respectively. The longitudinal-mode structure of laser was monitored by a F-P interferometer with FSR of 750 MHz and the result was depicted in inset of Fig. 3, which showed that the laser can operate with stable SLM. The transverse-mode characteristics of the output laser beam was also measured by a M^2 beam quality analyzer (M2SETVIS, Thorlabs), and the result was shown in Fig. 4. The measured values of M^2 at x and y axes were 1.07 and 1.06, respectively.

The tuning ability of IE was firstly inspected by rotating its incident angle, which was implemented by continuously varying the voltage supplied to GC. In this case, the output wavelength

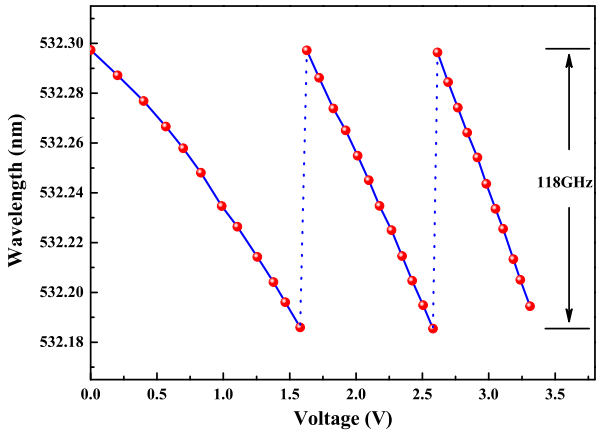

Fig. 5. The measured tuning range of the IE.

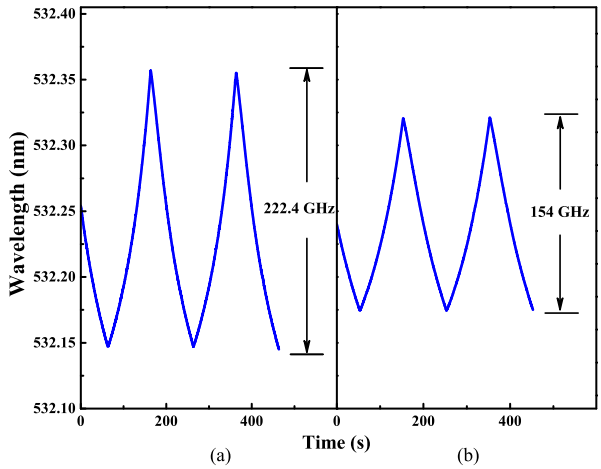

Fig. 6. The continuous tuning range of the CW single-frequency laser combining the locked IE and nonlinear loss with different L and η: (a) $L = 5.8\%$ and $\eta = 1.87\%$, (b) $L = 9.8\%$ and $\eta = 1.2\%$.

of laser was finely tuned and the recorded results by WLM were shown in Fig. 5. The abscissa axis in Fig. 5 stood for the voltage supplied to GC, which was corresponding to the incident angle of IE. It showed that the output wavelength of laser shifted toward the side of short-wave with the increasing of the voltage supplied to GC. When the voltage supplied to GC was raised to 1.579 V, the output wavelength of the laser was shifted to 532.1860 nm and then rapidly jumped to 532.2972 nm. With the same way, when the voltage supplied to GC was raised to 2.58 V, the output wavelength of laser jumped from 532.1855 nm to 532.2964 nm. The experimental results illustrated that FSR of IE was 59 GHz. Substituting the measured FSR of 59 GHz and other parameters including the gain linewidth 255 GHz of Nd:YVO_4 crystal, the intracavity linear loss (L) of 5.8% and SH conversion efficiency (η) of 1.87% to (4), the calculated maximal frequency-tuning ranges for the FW and SH wave lasers were 126.18 GHz and 252.36 GHz, respectively.

The expansibility of the nonlinear loss was verified after the transmission peak of IE was locked to the oscillating mode of the laser. Firstly, the output wavelength of laser was discretionarily tuned to 532.2549 nm by rotating its incident angle, which was implemented by modifying the voltage supplied to GC to 2.012 V. At that time, a modulation signal supplied by SC with the amplitude and frequency of 250 V and 10 kHz, respectively, was loaded onto the two electrodes mounted on the IE to modulate the light field of the intracavity FW. The generated 1064 nm laser leaked from the M_4 was separated from the main 532 nm laser by M_5 and directly detected by the broadband PD. The error signal was extracted by mixing the detected signal of PD with the low-voltage modulation signal. The obtained error signal was amplified and integrated with the suitable time constant and imported into the GC to control the incident angle of the IE. By optimizing the phase of the modulation signal, the transmission peak of the IE could be stably locked to the oscillating mode of the laser. Then the frequency of the output laser was continuously tuned by scanning the cavity length of the laser resonator, which was implemented by loading a high-voltage scanning signal with amplitude and frequency of 220 V and 5 mHz, respectively, onto the PZT adhered to M_3. At that case, the displacement of the PZT was about 70 μm. The experimental result was illustrated in Fig. 6(a). It was clear that the output wavelength of the laser was continuously tuned from 532.1471 nm to 532.3570 nm and the obtained maximal continuous frequency-tuning range was 222.4 GHz. During the continuous frequency tuning of the laser, the fluctuation of its output power was recorded from 1.22 W to 2.12 W. The experimentally obtained maximal continuous frequency-tuning range was narrower than calculated 253.36 GHz, which resulted from the deviations of the parameter values between experiment and theoretical calculation, especially the SH conversion efficiency, owing to the widely frequency scanning would lead to slightly phase mismatching of the nonlinear crystal and the SH conversion efficiency was minished instead of a certain value. In the experiment, to reduce the influence of the ambient temperature drift on the laser frequency drift, the whole elements of the laser resonator were mounted in a monoblock construction, whose temperature was controlled by a temperature controller with the accuracy of 0.02 °C. And the influence of the adopted PZT on the laser frequency drift was further estimated. Referring to the properties of the PZT, its coefficient of thermal expansion and length were -5 ppm/°C and 55 mm, respectively, so the estimated laser frequency drift caused by the PZT was about 17 MHz within the temperature drift range of 0.02 °C. The frequency drift of the output laser at 532 nm was also monitored and the measured result was 30 MHz within 1 min.

In order to verify the effectivity of the present method further, we intentionally modified the ratio of the intracavity linear loss (L) to the SH conversion efficiency (η) by replacing the mirror M_2 with another plane mirror coated with partial transmission film at 1064 nm with the transmission of 4% and maintaining the rest of the laser system unchanged. Under these conditions, the intracavity linear loss (L) was modified to 9.8%. When the pump power was 6.7 W, the output powers of 1.8 W and 0.54 W at 1064 nm and 532 nm respectively were obtained and the SH conversion efficiency (η) of 1.2% was estimated. The other parameters of the laser system were identical with that of the previous experiment. Substituting these parameters to (4), the maximal continuous frequency-tuning range of 178.12 GHz at

532 nm was calculated. In experiment, after the transmission peak of the IE was locked to the oscillating mode of the laser and the voltage loaded onto the PZT was continuously scanned, the maximal continuous frequency-tuning range of 154 GHz at 532 nm was implemented as shown in Fig. 6(b). The results distinctly notarized the expansion of the nonlinear loss on the continuous tuning range of the single-frequency laser.

V. Conclusion

In conclusion, we presented a new effective method of expanding the continuous frequency-tuning range of laser, which was implemented by combining a locked IE and a nonlinear loss element. Using a CW single-frequency and frequency-doubling laser with a LBO crystal to be both the frequency doubler and nonlinear loss element, the limitation of FSR of IE was broken through. It is expected that maximal tuning range covering whole gain linewidth of the gain medium can be reached by choosing suitable IE and nonlinear loss element according to (4). The presented method provides a feasible reference to develop different kinds of tunable single-frequency lasers with broadband continuous tuning range. Once the gain medium is determined, a suitable nonlinear crystal with larger nonlinear conversion coefficient d_{eff} and wider nonlinear spectral bandwidth should be adopted and an etalon with suitable thickness calculated by (4) can be selected.

References

[1] J. Laurat, T. Coudreau, G. Keller, N. Treps, and C. Fabre, "Compact source of Einstein-Podolsky-Rosen entanglement and squeezing at very low noise frequencies," *Phys. Rev. A*, vol. 70, Oct. 2004, Art. no. 042315.

[2] H. Vahlbruch *et al.*, "Observation of Squeezed Light with 10-dB Quantum-Noise Reduction," *Phys. Rev. Lett.*, vol. 100, Jan. 2008, Art. no. 033602.

[3] M. Chen, N. C. Menicucci, and O. Pfister, "Experimental realization of multipartite entanglement of 60 modes of a quantum optical frequency comb," *Phys. Rev. Lett.*, vol. 112, Mar. 2014, Art. no. 120505.

[4] A. Arie and R. L. Byer, "Laser heterodyne spectroscopy of $^{127}I_2$ hyperfine structure near 532 nm," *J. Opt. Soc. Amer. B*, vol. 10, pp. 1990–1997, Nov. 1993.

[5] F. Hong, J. Ye, L. Ma, S. Picard, C. J. Borde, and J. L. Hall, "Rotation dependence of electric quadrupole hyperfine interaction in the ground state of molecular iodine by high-resolution laser spectroscopy," *J. Opt. Soc. Amer. B*, vol. 18, pp. 379–387, Mar. 2001.

[6] J. Hamson, A. Finch, J. H. Flint, and P. F. Moulton, "Broad-band rapid tuning of a single-frequency diode-pumped neodymium laser," *IEEE J. Quantum Electron.*, vol. 28, no. 4, pp. 1123–1130, Apr. 1992.

[7] D. Radnatarov, S. Kobtsev, S. Khripunov, and V. Lunin, "240-GHz continuously frequency-tuneable Nd:YVO4/LBO laser with two intra-cavity locked etalons," *Opt. Express*, vol. 23, pp. 27322–27327, Oct. 2015.

[8] W. Z. Wang, H. D. Lu, J. Su, and K. C. Peng, "Broadband tunable single-frequency Nd:YVO_4/LBO green laser with high output power," *Appl. Opt.*, vol. 52, pp. 2279–2285, Apr. 2013.

[9] Y. H. Zheng, H. D. Lu, Y. Li, K. S. Zhang, and K. C. Peng, "Broadband and rapid tuning of an all-solid-state single-frequency Nd:YVO_4 laser," *Appl. Phys. B*, vol. 90, pp. 485–488, Jan. 2008.

[10] P. X. Jin, H. D. Lu, Y. X. Wei, J. Su, and K. C. Peng, "Single-frequency CW Ti:sapphire laser with intensity noise manipulation and continuous frequency-tuning," *Opt. Lett.*, vol. 42, pp. 143–146, Jan. 2017.

[11] K. I. Martin, W. A. Clarkson, and D. C. Hanna, "Self-suppression of axial mode hopping by intracavity second-harmonic generation," *Opt. Lett.*, vol. 22, pp. 375–377, Mar. 1997.

[12] H. D. Lu, J. Su, Y. H. Zheng, and K. C. Peng, "Physical conditions of single-longitudinal-mode operation for high-power all-solid-state lasers," *Opt. Lett.*, vol. 39, pp. 1117–1120, Mar. 2014.

[13] S. Greenstein and M. Rosenbluh, "The influence of nonlinear spectral bandwidth on single longitudinal mode intra-cavity second harmonic generation," *Opt. Commun.*, vol. 248, pp. 241–248, Apr. 2005.

[14] H. D. Lu, X. J. Sun, M. H. Wang, J. Su, and K. C. Peng, "Single frequency Ti:sapphire laser with continuous frequency-tuning and low intensity noise by means of the additional intracavity nonlinear loss," *Opt. Express*, vol. 22, pp. 24551–24558, Oct. 2014.

[15] C. W. Zhang, H. D. Lu, Q. W. Yin, and J. Su, "Continuous-wave single-frequency laser with dual wavelength at 1064 and 532 nm," *Appl. Opt.*, vol. 53, pp. 6371–6374, Oct. 2014.

[16] H. D. Lu and K. C. Peng, "Realization of the single-frequency and high power as well as frequency-tuning of the laser by manipulating the nonlinear loss," *J. Quantum Opt.*, vol. 21, pp. 171–176, May 2015.

[17] P. X. Jin, H. D. Lu, J. Su, and K. C. Peng, "Scheme for improving laser stability via feedback control of intracavity nonlinear loss," *Appl. Opt.*, vol. 55, pp. 3478–3482, May 2016.

Pixian Jin was born in 1989. He received the Master's degree in optical engineering, in 2014, from Shanxi University, Taiyuan, China, where he is currently working toward the Ph.D. degree in optics at the Institute of Opto-Electronics, Shanxi University.

His current research interests include all-solid-state laser technology, tunable optics devices, and optoelectronic technology.

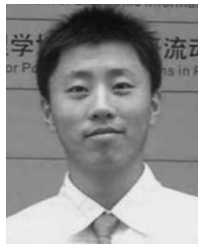

Huadong Lu was born in 1981. He received the Ph.D. degree in laser technology from Shanxi University, Taiyuan, China, in 2011.

He is a currently an Associate Professor with the Institute of Opto-Electronics, Shanxi University. His research interests include all-solid-state laser technology, quantum optics devices, and tunable optics devices.

Qiwei Yin was born in 1985. He received the Ph.D. degree in optics from Shanxi University, Taiyuan, China, in 2016.

He is currently an Engineer with the Institute of Opto-Electronics, Shanxi University. His current research focuses on the high-power all-solid-state single-frequency lasers.

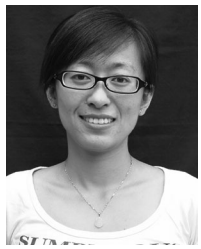

Jing Su was born in 1979. She received the Ph.D. degree in physics from Nankai University, Tianjin, China, in 2007.

She is a currently an Associate Professor with the Institute of Opto-Electronics, Shanxi University, Taiyuan, China. Her research interests include all-solid-state laser technology, quantum optics devices, and tunable optics devices.

Kunchi Peng was born in 1936. He received the B.S. degree in physics from Sichuan University, Chengdu, China, in 1961.

He was a Visiting Scholar with Paris 11th University, Orsay, France, The University of Texas at Austin, Austin, TX, USA, and the California Institute of Technology, Pasadena, Pasadena, CA, USA, from 1980 to 1982, 1982 to 1984, and 1988 to 1989, respectively. Since 1990, he has been a Professor with the Institute of Opto-Electronics, Shanxi University, Shanxi, China. His research interests include all-solid-state laser technology, quantum information networks, and quantum optics devices.

Prof. Peng was elected as a Fellow of the Optical Society of America in April 2006 and is a member of the Chinese Physical Society.